JVSTA Journal of Vacuum Science & Technology A

Controllable nitrogen doping in as deposited TiO2 film and its effect on post deposition annealing

Shaoren Deng, Sammy W. Verbruggen, Silvia Lenaerts, Johan A. Martens, Sven Van den Berghe, Kilian Devloo-Casier, Wouter Devulder, Jolien Dendooven, Davy Deduytsche, and Christophe Detavernier

Citation: Journal of Vacuum Science & Technology A **32**, 01A123 (2014); doi: 10.1116/1.4847976
View online: http://dx.doi.org/10.1116/1.4847976
View Table of Contents: http://scitation.aip.org/content/avs/journal/jvsta/32/1?ver=pdfcov
Published by the AVS: Science & Technology of Materials, Interfaces, and Processing

Re-register for Table of Content Alerts
Create a profile.
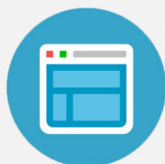
Sign up today!

Redistribution subject to AVS license or copyright; see http://scitation.aip.org/termsconditions. Download to IP: 134.58.253.57 On: Mon, 10 Mar 2014 13:00:41

CrossMark

Controllable nitrogen doping in as deposited TiO_2 film and its effect on post deposition annealing

Shaoren Deng
Department of Solid State Sciences, Ghent University, Krijgslaan 281/S1, B-9000 Gent, Belgium

Sammy W. Verbruggen
Department of Bio-Engineering Sciences, University of Antwerp, Groenenborgerlaan 171, B-2020 Antwerp, Belgium and Center for Surface Chemistry and Catalysis, KU Leuven, Kasteelpark Arenberg 23, B-3001 Heverlee, Belgium

Silvia Lenaerts
Department of Bio-Engineering Sciences, University of Antwerp, Groenenborgerlaan 171, B-2020 Antwerp, Belgium

Johan A. Martens
Center for Surface Chemistry and Catalysis, KU Leuven, Kasteelpark Arenberg 23, B-3001 Heverlee, Belgium

Sven Van den Berghe
SCK-CEN, Boeretang 200, B-2400 Mol, Belgium

Kilian Devloo-Casier, Wouter Devulder, Jolien Dendooven, Davy Deduytsche, and Christophe Detavernier[a)]
Department of Solid State Sciences, Ghent University, Krijgslaan 281/S1, B-9000 Gent, Belgium

(Received 4 September 2013; accepted 30 November 2013; published 13 December 2013)

In order to narrow the band gap of TiO_2, nitrogen doping by combining thermal atomic layer deposition (TALD) of TiO_2 and plasma enhanced atomic layer deposition (PEALD) of TiN has been implemented. By altering the ratio between TALD TiO_2 and PEALD TiN, the as synthesized TiO_xN_y films showed different band gaps (from 1.91 eV to 3.14 eV). *In situ* x-ray diffraction characterization showed that the crystallization behavior of these films changed after nitrogen doping. After annealing in helium, nitrogen doped TiO_2 films crystallized into rutile phase while for the samples annealed in air a preferential growth of the anatase TiO_2 along (001) orientation was observed. Photocatalytic tests of the degradation of stearic acid were done to evaluate the effect of N doping on the photocatalytic activity. © *2014 American Vacuum Society*. [http://dx.doi.org/10.1116/1.4847976]

I. INTRODUCTION

As a popular photocatalyst, TiO_2 has been widely used in pollutant degradation[1] or water splitting[2] in recent decades. However, its large band gap (3.2 eV) prevents TiO_2 to make efficient use of natural sunlight, since a large fraction of the photons in sunlight have a lower energy content than 3.2 eV. Nitrogen doping has been widely considered as an effective way to tune the band gap of TiO_2.[3] Several methods have been studied to introduce nitrogen into the lattice, such as annealing TiO_2 films in ammonia ambient,[4] ammonia plasma post treatment after TiO_2 synthesis,[5] applying ammonia plasma during chemical vapor deposition,[6] and so on. In virtue of its characteristic of self-limited growth, atomic layer deposition (ALD)[7–9] has demonstrated its merit of controllable synthesis of metal oxide nanolaminates and doped metal oxide layers such as Al doped ZnO.[10–12] Recently, two methods of incorporating nitrogen into TiO_2 by ALD have been demonstrated. Pore *et al.*[13] added nitrogen into a TiO_2 film by using thermal TiO_2 and TiN ALD processes. For example, after every five cycles of TiO_2, one cycle of TiN was inserted. Chen *et al.*[14] incorporated nitrogen into a TiO_2 film by using an ammonia solution as a reactant during the ALD process. Here we introduce a new method for controllable nitrogen doping by combing thermal ALD (TALD) and plasma enhanced ALD (PEALD).

II. EXPERIMENT

The nitrogen doped TiO_2 (N-TiO_2) films were grown on Si (100) substrates at 150 °C in a homemade ALD system with base pressure below 10^{-6} mbar.[15] In the ALD process, tetrakis dimethylamido titanium (TDMAT) (Sigma Aldrich, 99.99%) was used as Ti source while water and ammonia plasma were employed as oxygen and nitrogen sources, respectively. A duration of 5 s was used for each pulse. The pulse pressures of TDMAT and water were about $5*10^{-3}$ mbar. The ammonia plasma pulse of $7*10^{-3}$ mbar was generated by a 300 W remote RF plasma generator. In order to introduce different amounts of nitrogen doping in TiO_2, TALD TiO_2 and PEALD TiN cycles were alternated. Every 2, 5, or 9 cycles of TALD TiO_2, one PEALD TiN cycle was inserted. For every deposition, TALD TiO_2 was the very first cycle. The total numbers of ALD cycles for these samples were $167 \times (2+1)$, $83 \times (5+1)$, and $50 \times (9+1)$, respectively. So, in total, ~500 ALD cycles were applied. We will further denote these samples as N-TiO_2-2:1, N-TiO_2-5:1, and N-TiO_2-9:1. Five hundred cycles pure TiO_2 and TiN were also deposited as references. To determine the band gaps by UV-VIS transmission measurements, the N-TiO_2

a)Electronic mail: Christophe.Detavernier@ugent.be

Redistribution subject to AVS license or copyright; see http://scitation.aip.org/termsconditions. Download to IP: 134.58.253.57 On: Mon, 10 Mar 2014 13:00:41

films were deposited on quartz substrates. X-ray photoelectron spectroscopy (XPS) was performed using Al Kα x-rays. XPS spectra were measured for each element by accumulating 30 scans in 0.1 eV steps with 0.1 s collection time per step, and calibrated using the C1s peak at 284.6 eV which is attributed to the adventitious carbon on the surface of the sample. The passing energy was 10 eV for each element being investigated. X-ray reflectivity (XRR) was measured using a Bruker D8 Discover system. *In situ* x-ray diffraction (XRD) was carried out in a home modified Bruker D8 Discover system with copper Kα source to investigate the crystallization behavior of the films during annealing in air and He ambients.[16] Atomic force microscopy (AFM) characterization was carried out using a Bruker Dimension Edge system. A 5 μm by 5 μm area of the sample was measured in order to calculate the root mean square (RMS) roughness. After annealing at 550 °C in air and 650 °C in He ambient for 3 h, respectively, the photocatalytic activities of the annealed N-TiO_2 films toward the degradation of a solid layer of stearic acid (SA) were measured. All samples were spin coated with 100 μL of a 0.25 wt. % SA solution in chloroform at 1000 rpm for 1 min. After spin coating, all samples were dried in a furnace at 70 °C for 10 min and finally left open to the ambient for at least 1 h to establish equilibrium with the test environment before the actual photocatalytic measurement. The efficiency of the samples was measured under UV (385 nm LEDs) as well as visible light (420 nm LEDs) illumination. The disappearance of SA during illumination was measured by taking Fourier transform infrared spectroscopy absorbance spectra of the solid film, and plotting the integrated area of the IR band between 2800 and 3000 cm^{-1}, which are ascribed to three different C-H vibrations of SA.[17,18]

III. RESULTS AND DISCUSSION

The optical picture in Fig. 1 demonstrates a color change of the different samples, giving the first indication that the N doping affects the optical properties of the films. Transmission measurements on these as deposited N-TiO_2 films [Fig. 2(a)] show that the absorption edge gradually shifts from ~350 nm for pure TiO_2 to ~500 nm for N-TiO_2-2:1. The band gaps of the as deposited N-TiO_2 films can be extracted from a Tauc plot by plotting $(\alpha h\nu)^{1/2}$ against the photon energy $h\nu$ [Fig. 2(b)].[19] The gradually decreasing band gaps from 3.14 eV to 1.91 eV of the as deposited films confirm the controllable nitrogen doping into the as deposited film. It is worth to mention that a sample of N-TiO_2-2:1 prepared by combining TALD TiO_2 and TALD TiN was also tested and no band gap narrowing was observed. This result which is not in agreement with the previous work by Pore *et al.*,[13] could be due to the difference in Ti precursors and/or the design of the ALD tool.

Physical characterization of the nitrogen doped films was performed by XPS, XRR, XRD, and AFM. After slightly argon milling the top surface, XPS characterization on the as deposited N-TiO_2-2:1 sample further confirms the successful doping of nitrogen into the as deposited films (Fig. 3). Two peaks located at 396.3 eV and 397.2 eV were fitted to the N1s spectrum by using a Shirley background. The nitrogen in the film consisted of substitutional N bonded with Ti^{4+} and N bonded to Ti^{3+} as TiN_x. Figures 3(b) and 3(c) show the XPS spectra of O1s and Ti2p. The broad peak in the spectrum of $Ti2p^{2/3}$ confirms that Ti atoms in the sample have both 4+ and 3+ sates. The fitted peak located at 530.7 eV in the O1s spectrum indicates oxygen vacancies

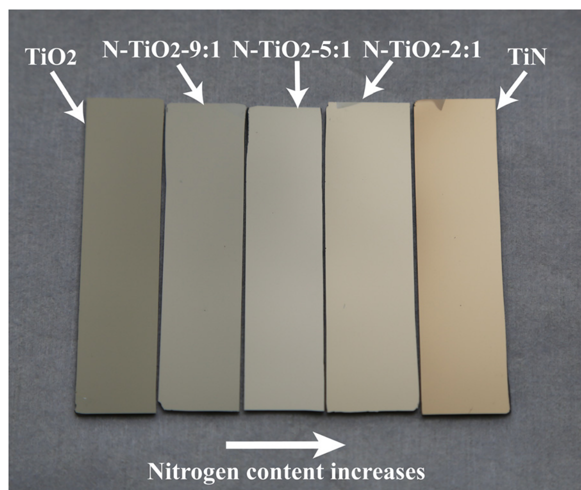

Fig. 1. (Color online) Optical image of N-TiO_2 samples.

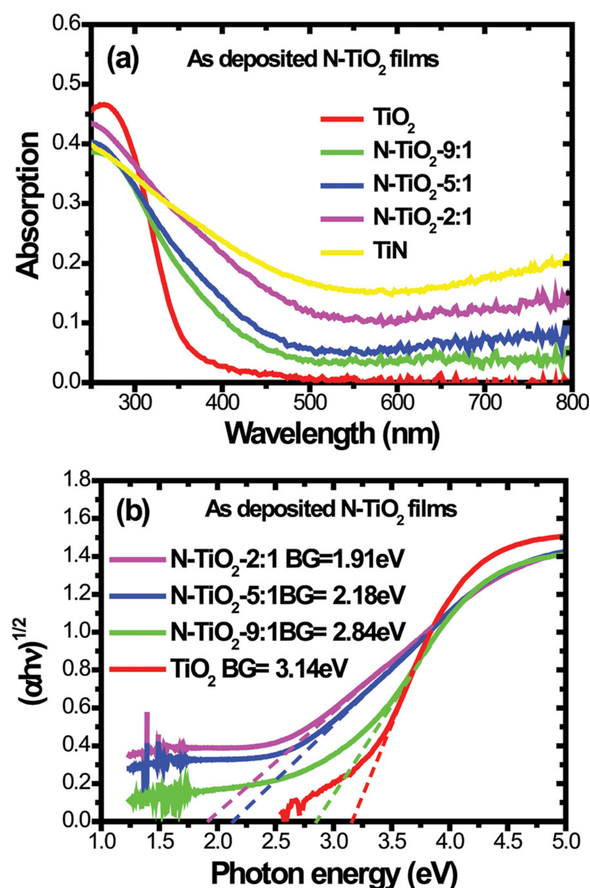

Fig. 2. (Color online) (a) Transmission measurement on as deposited N-TiO_2 films. (b) Tauc plotting of the transmission data for the as deposited N-TiO_2 films. The fitted band gaps (BG) are indicated in the legend.

Redistribution subject to AVS license or copyright; see http://scitation.aip.org/termsconditions. Download to IP: 134.58.253.57 On: Mon, 10 Mar 2014 13:00:41

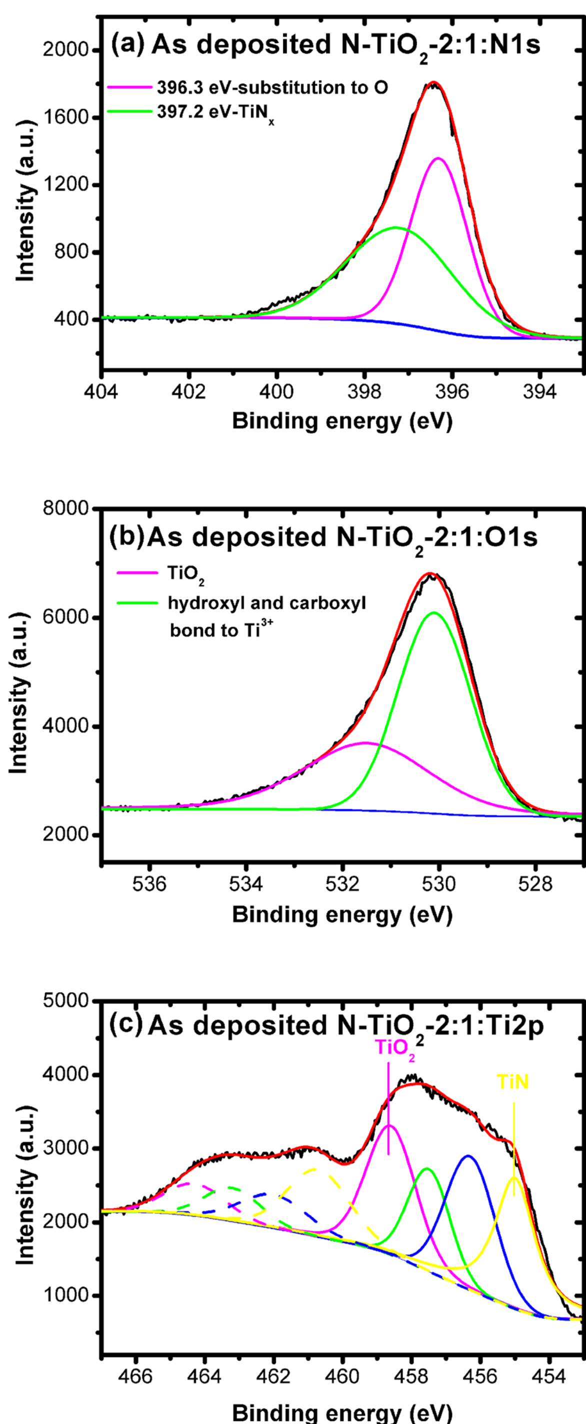

FIG. 3. (Color online) XPS spectra of (a) N1s, (b) O1s, and (c) Ti2p of as deposited $N\text{-}TiO_2$-2:1 sample.

and/or absorbed hydroxyl and carboxyl species. The peaks located at 457.4 and 456.2 eV in the Ti2p spectrum could be assigned to oxynitride species, in agreement with previous observations.[5]

Table I summarizes the results of XPS, XRR, and AFM measurements. As the ratio between PEALD and TALD increases from 0 to 1:2, the nitrogen content gradually increases from 0.8 at. % to 9.4 at. %, resulting in a narrowing of the band gap from 3.14 eV to 1.91 eV. The nitrogen content in the pure TiO_2 might be due to the nitrogen from the TDMAT precursor, which might not be completely removed during the deposition. The thicknesses of the as deposited $N\text{-}TiO_2$ films vary from 21.5 nm to 34.8 nm, which is caused by a difference in growth rates. For TALD TiO_2 process and PEALD TiN process at 150 °C, the growth rates are ~0.4 Å per cycle and ~0.7 Å per cycle, respectively.[20] The RMS roughness of the as deposited samples in Table I indicates that nitrogen doping slightly increases the roughness when compared to the reference samples of pure TiO_2 and TiN. *Ex situ* XRD characterization on the films (Fig. 4) indicates that for pure TiO_2 and low doped $N\text{-}TiO_2$, the as deposited films are not crystalline. Highly doped $N\text{-}TiO_2$-2:1 shows two minor diffraction peaks from TiN (111) and TiN (200).

TABLE I. Nitrogen content measured by XPS, thicknesses measured by XRR and the roughnesses determined by AFM of the as deposited TiO_2, TiN, and $N\text{-}TiO_2$ films.

Sample	Nitrogen content (at. %)	Thickness	RMS roughness (nm)
TiN	46.4	34.8	0.17
$N\text{-}TiO_2$-2:1	9.4	25.1	0.33
$N\text{-}TiO_2$-5:1	4.7	22.2	0.27
$N\text{-}TiO_2$-9:1	3.3	21.9	0.32
TiO_2	0.8	21.5	0.26

For photocatalytic applications, TiO_2 needs to be crystalline.[21] Therefore, it is important to investigate the crystallization behavior of these as deposited $N\text{-}TiO_2$ films. *In situ* XRD characterization was employed to investigate the crystallization behavior of $N\text{-}TiO_2$ films during annealing in He and air ambient. Figure 5 shows the evolution of the x-ray diffraction as a function of annealing temperature over a two theta range of 20°. The diffracted intensity is plotted as a gray scale, with black as the background. As shown in Fig. 5(a), when $N\text{-}TiO_2$ films are annealed in He from 20 °C to 900 °C at a rate of 5 °C/min, all the $N\text{-}TiO_2$ films crystallize into the rutile phase, as evidenced by the appearance of rutile (110) and (101) diffraction peaks. Only the pure TiO_2 film crystallizes into the anatase phase in He ambient, as evidenced by the anatase (101) peak. The crystallization temperature of $N\text{-}TiO_2$ also shifts from 520 °C to 630 °C as the nitrogen contents increases. When $N\text{-}TiO_2$ samples are

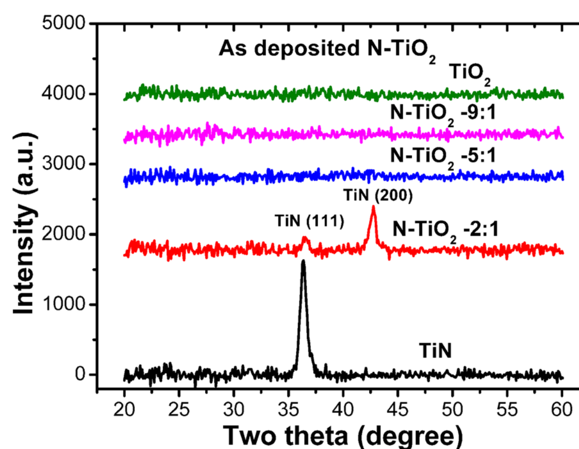

FIG. 4. (Color online) XRD patterns of the as deposited $N\text{-}TiO_2$ films.

Redistribution subject to AVS license or copyright; see http://scitation.aip.org/termsconditions. Download to IP: 134.58.253.57 On: Mon, 10 Mar 2014 13:00:41

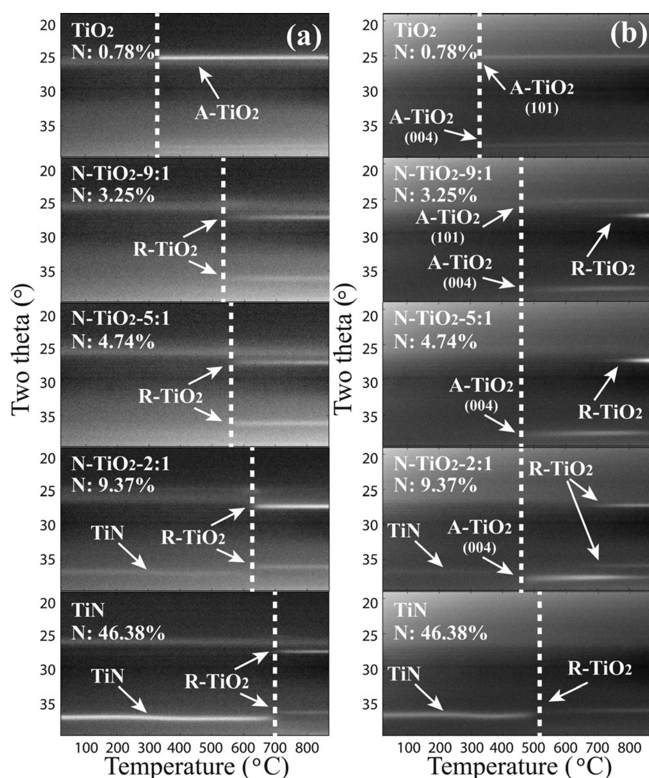

FIG. 5. (a) *In situ* XRD characterizations of N-TiO_2 films during annealing in He ambient from 20 °C to 900 °C. (b) *In situ* XRD characterizations of N-TiO_2 films during annealing in air ambient from 20 °C to 900 °C. A-TiO_2 and R-TiO_2 stand for anatase and rutile TiO_2, respectively.

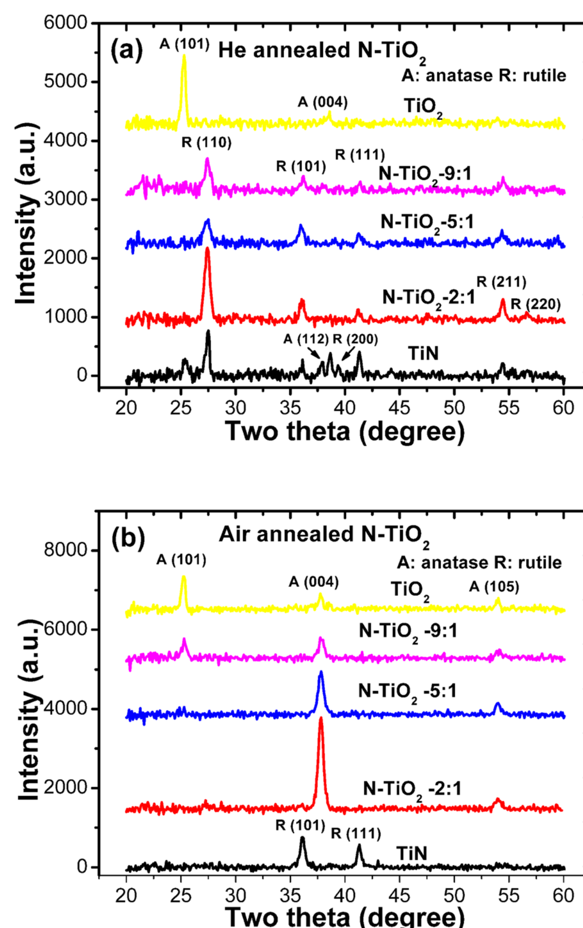

FIG. 6. (Color online) (a) *Ex situ* XRD patterns of N-TiO_2 films annealed in He at 650 °C for 3 h. (b) *Ex situ* XRD patterns of N-TiO_2 films annealed in air at 550 °C for 3 h.

annealed in air [Fig. 5(b)], they all crystallize into anatase at 460 °C, compared to 340 °C for pure TiO_2 and 510 °C for TiN. Interestingly, in Fig. 5(b), sample N-TiO_2-2:1 and 5:1 only show the (004) diffraction peak of anatase before the rutile phase appears at higher temperature. For pure TiO_2 and N-TiO_2-9:1, both diffraction peaks of anatase (101) and (004) are observed simultaneously at 340 °C and 460 °C, respectively.

Based on the *in situ* XRD measurement, we decided to further investigate the crystallinity of samples that were annealed for 3 h at 650 °C in He ambient and at 550 °C in air ambient, respectively. *Ex situ* Bragg-Brentano XRD characterization in Fig. 6 illustrates the different crystallization behaviors. An offset of 5° was taken during the measurement to avoid the diffraction peak from the silicon substrate. As can be seen in Fig. 6(a), all N-TiO_2 films crystallize into the rutile phase. As the amount of nitrogen decreases, the intensity of the rutile (110) diffraction peak slightly decreases. In Fig. 6(b), N-TiO_2-2:1 and 5:1 only show a strong diffraction peak of anatase (004) and a minor peak of (105) when annealed in air. As the nitrogen content decreases, the (004) peak weakens and the (101) peak appears in sample N-TiO_2-9:1. This indicates a textured growth of TiO_2 with preferential (001) orientation for heavily N doped samples. This preferential orientation may be due to the difference between relaxed and unrelaxed TiO_2 films.[22,23] For the relaxed pure TiO_2 film, the (101) plane has the lowest surface energy. However, for N-TiO_2, the incorporation of nitrogen introduces strain in the lattice and results in the lowest surface energy on the (001) plane. A similar dopant-induced texturing effect was previously observed by Ali *et al.*[24] in neodymium doped TiO_2 film. The different phases that the N-TiO_2 films transform to also imply that the annealing ambient strongly affects the crystallization process. The lack of oxygen in the He annealing process results in the formation of rutile phase while the oxygen-rich ambient results in the formation of a textured anatase phase.

Optical transmission measurements on the N-TiO_2 samples after annealing in Fig. 7 show that the annealing process eliminates the effect of nitrogen doping on the band gap. The absorption edges for all the N-TiO_2 films shift back to ~350 nm. In Fig. 8, XPS characterization on N-TiO_2-2:1 samples annealed in air and He proves the loss of nitrogen from the samples. For the N-TiO_2-2:1 annealed in air, no N 1 s peak could be observed on the surface of the film. The nitrogen content inside the film detected by XPS after argon milling was about 1.2 at. %, which is inadequate to narrow the band gap significantly. For the sample annealed in He ambient, a minor nitrogen peak around 399–403 eV could still be observed. This minor peak could be assigned to interstitial nitrogen in the film, which is also observed in the pure TiO_2 and other N-TiO_2 films.[5] The nitrogen content after

Redistribution subject to AVS license or copyright; see http://scitation.aip.org/termsconditions. Download to IP: 134.58.253.57 On: Mon, 10 Mar 2014 13:00:41

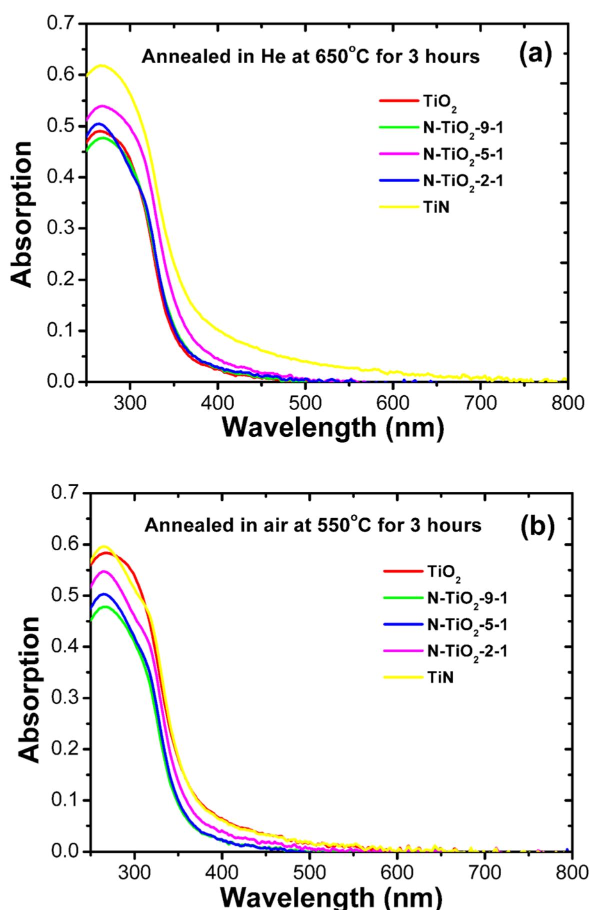

FIG. 7. (Color online) Transmission measurements on (a) N-TiO_2 films annealed in He at 650 °C for 3 h and (b) N-TiO_2 films annealed in air at 550 °C for 3 h.

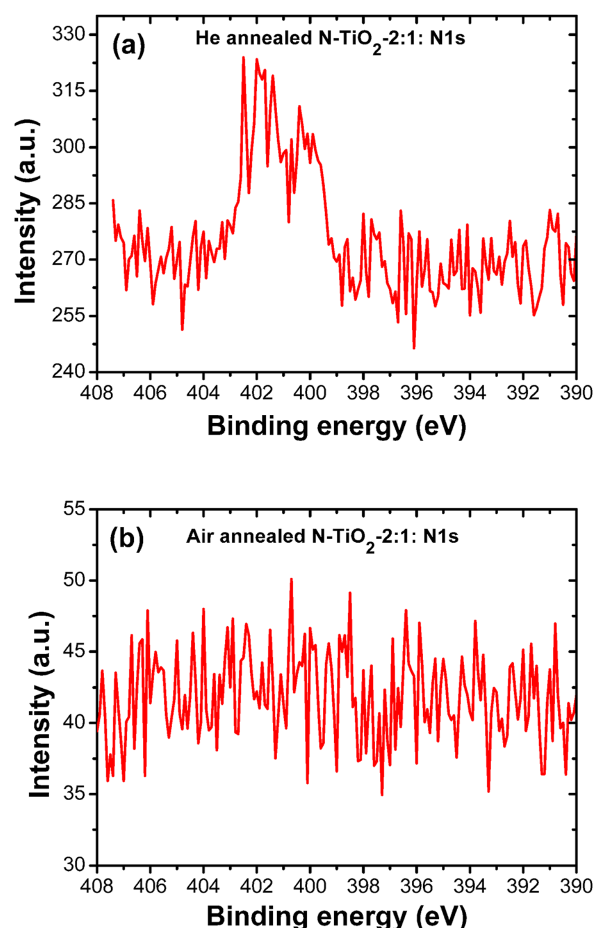

FIG. 8. (Color online) N 1s XPS spectra of (a) N-TiO_2 films annealed in He at 650 °C for 3 hours and (b) N-TiO_2 films annealed in air at 550 °C for 3 hours.

annealing in He is lower than 1 at. % and not enough to effectively narrow the band gap. The elimination of nitrogen implies that nitrogen is not very stable at the elevated temperatures required to crystallize the as deposited films. After annealing, the roughness of the annealed nitrogen doped samples and TiN sample increased compared to the as deposited samples. Figures 9(a) and 9(b) show the AFM images of the N-TiO_2-2:1 sample before and after annealing in air. The RMS roughnesses of the N-TiO_2-9:1, N-TiO_2-5:1, N-TiO_2-2:1, and TiN samples increased to 0.58, 0.57, 0.86, and 0.68 nm after annealing in air, while the RMS roughness of the reference TiO_2 sample remained about the same after the annealing. After annealing in He, the surface roughness of N-TiO_2 increased dramatically [Fig. 9(c)]. The surface roughness of N-TiO_2-9:1, N-TiO_2-5:1, and N-TiO_2-2:1was 0.46 nm, 2.97 nm, and 10.9 nm, respectively. The roughness of reference TiO_2 and TiN samples was 0.32 nm and 3.08 nm, respectively. The higher surface roughness of the samples than annealed in He can be related to the higher annealing temperature. Second, for the N-TiO_2 samples, the less nitrogen content in the film, the smoother the surface after annealing in He. This suggests that the removal of the N also plays an important role in the final surface roughness.

In order to evaluate the effect of nitrogen doping on the photocatalytic activity, the photocatalytic degradation of a solid layer of SA was investigated under UV and visible light illumination. The formal quantum efficiency (FQE) is used to evaluate the activities of the annealed N-TiO_2 layers. FQE is defined as the rate of SA degradation in molecules/cm^2/s over the rate of incident light in photons/cm^2/s. Figure 10(a) shows that the FQEs of annealed N-TiO_2 samples under UV light are slightly higher than that of pure TiO_2, irrespective of the annealing conditions (air or He). The air annealed pure TiN film shows the highest activity, which is 55% higher compared to N-TiO_2-2:1 and 127% higher compared to pure TiO_2, despite the fact that the latter consists of anatase, which is commonly regarded as the most photoactive form of TiO_2. A possible explanation for this observation could be that the roughness of the TiN film after the annealing is significantly higher than that of the TiO_2 film. Also, the thickness of the film plays an important role.[25] To investigate the effect of film thickness, a TiN sample with a similar thickness (300 ALD cycles, ~19.5 nm) as that of TiO_2 film was prepared and annealed in both He and air. The photocatalytic test result of this film shows that the photoactivity of the thinner TiN film after annealing only amounts to one third of the activity of the TiO_2 film under UV illumination, which evidences the high FQE of the original annealed TiN sample. The FQEs under visible light

Redistribution subject to AVS license or copyright; see http://scitation.aip.org/termsconditions. Download to IP: 134.58.253.57 On: Mon, 10 Mar 2014 13:00:41

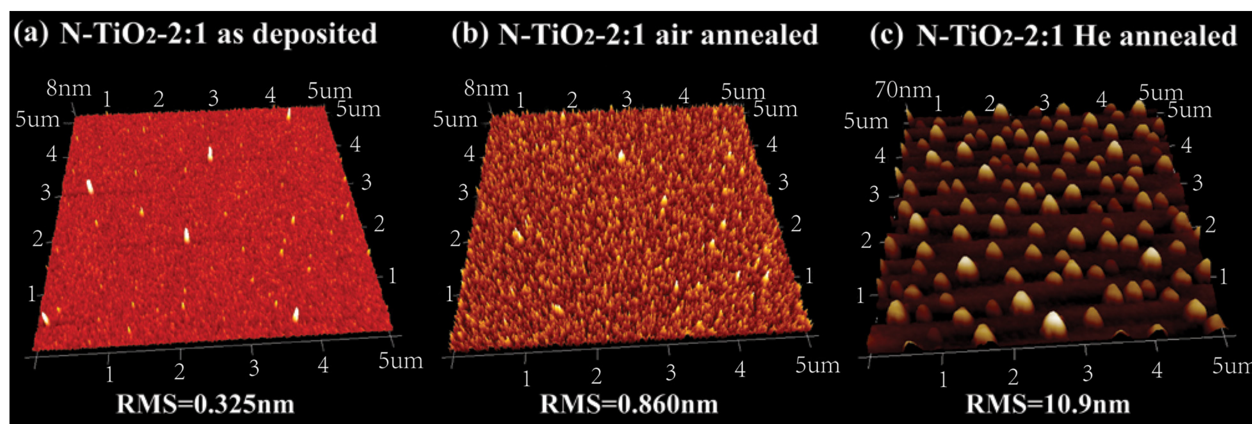

FIG. 9. (Color online) AFM images of N-TiO_2-2:1 sample (a) as deposited, (b) after annealing in air and (c) annealed in He.

illumination (420 nm LEDs) are shown in Fig. 10(b) and are approximately one order of magnitude lower than those obtained under UV light, leading to the conclusion that the loss of nitrogen during annealing limits the photocatalytic activity under visible light. This is supported by the observation that nitrogen doped TiO_2 films are unstable when annealed at higher temperature as required for crystallization. This could be potentially solved by directly depositing crystallized TiO_2 films, e.g., by using a Ti precursor with a higher decomposition temperature such as $TiCl_4$. For the TDMAT precursor used in our case, the highest deposition temperature is limited to 150 °C, which results in an amorphous as deposited film.

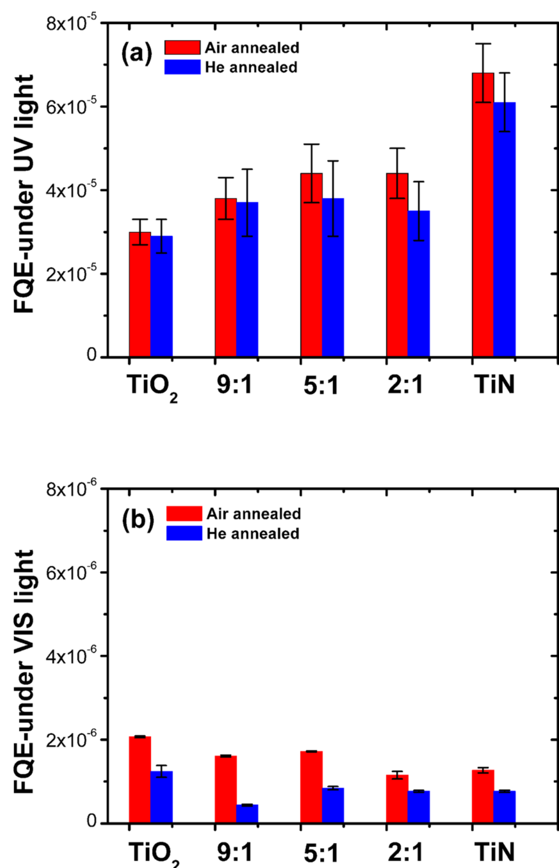

FIG. 10. (Color online) FQEs for photocatalytic degradation of SA for N-TiO_2 films annealed in He and air under (a) UV light and (b) visible light.

IV. CONCLUSIONS

To conclude, a new method combing TALD TiO_2 and PEALD TiN was proposed for the incorporation of nitrogen into TiO_2 films. The controllable nitrogen doping strategy resulted in a tunable band gap narrowing for the as deposited film. The investigation of the post deposition annealing step revealed that nitrogen doped TiO_2 could be crystallized into the rutile phase when annealed in He ambient while an anatase (001) textured growth was observed when annealed in air. The photocatalytic measurements showed that even though annealed N-TiO_2 samples lost most of the doped nitrogen and showed no significant activities under visible light, the N-TiO_2 samples still showed higher activity than a pure TiO_2 film under UV light, which was probably due to the increased surface roughness after annealing and the larger film thickness.

ACKNOWLEDGMENTS

The authors wish to thank the Research Foundation–Flanders (FWO) for financial support. The authors acknowledge the European Research Council for funding under the European Union's Seventh Framework Programme (FP7/2007-2013)/ERC grant agreement Nos. 239865-COCOON and 246791-COUNTATO. The authors also acknowledge the support from UGENT-GOA-01G01513 and IWT-SBO SOSLion. J.A.M. acknowledges the Flemish government for long-term structural funding (Methusalem). J.D. acknowledges the Flemisch FWO for a postdoctoral fellowship.

[1]S. Kwon, M. H. Fan, A. T. Cooper, and H. G. Yang, Crit. Rev. Environ. Sci. Technol. **38**, 197 (2008).
[2]M. Ni, M. K. H. Leung, D. Y. C. Leung, and K. Sumathy, Renewable Sustain. Energy Rev. **11**, 401 (2007).
[3]M. Pelaez *et al.*, Appl. Catal. B: Environ. **125**, 331 (2012).
[4]H. Wang, G. Wang, Y. Ling, M. Lepert, C. Wang, J. Z. Zhang, and Y. Li, Nanoscale **4**, 1463 (2012).
[5]D. J. V. Pulsipher, I. T. Martin, and E. R. Fisher, ACS Appl. Mater. Interfaces **2**, 1743 (2010).
[6]S. Buzby, M. A. Barakat, H. Lin, C. Ni, S. A. Rykov, J. G. Chen, and S. Ismat Shah, J. Vac. Sci. Technol. B **24**, 1210 (2006).
[7]S. M. George, Chem. Rev. **110**, 111 (2010).

Redistribution subject to AVS license or copyright; see http://scitation.aip.org/termsconditions. Download to IP: 134.58.253.57 On: Mon, 10 Mar 2014 13:00:41

[8]C. Maichy, M. Bechelany, and N. Pinna, Adv. Mater. **24**, 1017 (2012).
[9]C. Detavernier, J. Dendooven, S. P. Sree, K. F. Ludwig, and J. A. Martens, Chem. Soc. Rev. **40**, 5242 (2011).
[10]V. Lujala, J. Skarp, M. Tammenmaa, and T. Suntola, Appl. Surf. Sci. **82–83**, 34 (1994).
[11]E. B. Yousfi, B. Weinberger, F. Donsanti, P. Cowache, and D. Lincot, Thin Solid Films **387**, 29 (2001).
[12]J. S. Na, G. Scarel, and G. N. Parsons, J. Phys. Chem. C **114**, 383 (2010).
[13]V. Pore, M. Heikkila, M. Ritala, M. Leskela, and S. Areva, J. Photochem. Photobiol. A **177**, 68 (2006).
[14]H. E. Cheng, W. J. Lee, C. M. Hsu, M. H. Hon, and C. L. Huang, Electrochem. Solid-State Lett. **11**, D81 (2008).
[15]Q. Xie, Y. L. Jiang, C. Detavernier, D. Deduytsche, R. L. Van Meirhaeghe, G. P. Ru, B. Z. Li, and X. P. Qu, J. Appl. Phys. **102**, 083521 (2007).
[16]W. Knaepen, S. Gaudet, C. Detavernier, R. L. Van Meirhaeghe, J. J. Sweet, and C. Lavoie, J. Appl. Phys. **105**, 083532 (2009).
[17]Y. Paz, Z. Luo, L. Rabenberg, and A. Heller, J. Mater. Res. **10**, 2842 (1995).
[18]A. Mills and J. S. Wang, J. Photochem. Photobiol. A: Chem. **182**, 181 (2006).
[19]J. Tauc, R. Grigorovici, and A. Vancu, Phys. Status Solidi B **15**, 627 (1966).
[20]J. Musschoot, Q. Xie, D. Deduytsche, S. Van den Berghe, R. L. Van Meirhaeghe, and C. Detavernier, Microelectron. Eng. **86**, 72 (2009).
[21]B.Ohtani, Y. Ogawa, and S. Nishimoto, J. Phys. Chem. B **101**, 3746 (1997).
[22]M. Lazzeri, A. Vittadini, and A. Selloni, Phys. Rev. B **63**, 155409 (2001).
[23]A. Vittadini, M. Casarin, and A. Selloni, Theor. Chem. Acc. **117**, 663 (2007).
[24]A. Ali, E. Yasitepe, I. Ruzybayev, S. Ismat Shah, and A. S. Bhatti, J. Appl. Phys. **112**, 113505 (2012).
[25]M. Heikkila, E. Puukilainen, M. Ritala, and M. Leskela, J. Photochem. Photobiol. A: Chem. **204**, 200 (2009).

Redistribution subject to AVS license or copyright; see http://scitation.aip.org/termsconditions. Download to IP: 134.58.253.57 On: Mon, 10 Mar 2014 13:00:41